Acta Pharmaceutica Sinica B 2025;15(3):1230−1241

Chinese Pharmaceutical Association
Institute of Materia Medica, Chinese Academy of Medical Sciences

Acta Pharmaceutica Sinica B

www.elsevier.com/locate/apsb
www.sciencedirect.com

ORIGINAL ARTICLE

Bispecific killer engager for targeted depletion of PD-1 positive lymphocytes: A new avenue for autoimmune disease treatment

Lauren C. Naatz[a], Shuyun Dong[a], Brian Evavold[b], Xiangyang Ye[c], Mingnan Chen[a,*]

[a]*Department of Molecular Pharmaceutics, University of Utah, Salt Lake City, UT 84112, USA*
[b]*Department of Pathology, University of Utah, Salt Lake City, UT 84112, USA*
[c]*Department of Pharmacotherapy, University of Utah, Salt Lake City, UT 84112, USA*

Received 30 May 2024; received in revised form 5 September 2024; accepted 6 September 2024

KEY WORDS

Immunotherapy;
Bispecific killer engager;
Bispecific antibody;
PD-1-positive cells;
Autoimmune disease;
Natural killer cell;
PD-1;
Antibody-dependent cellular cytotoxicity

Abstract Bispecific killer cell engagers (BiKEs) are a powerful tool to incite the killing power of natural killer (NK) cells. Here, we posited that the BiKE technology could be utilized to deplete activated immune cells expressing programmed death-1 (PD-1$^+$ cells), and hence treat autoimmune diseases since these cells drive the disorders. We designed and generated PD-1 BiKE that targets an activating NK cell receptor, CD16, and PD-1. PD-1 BiKE showed specific binding to PD-1$^+$ cells and engaged CD16 simultaneously. PD-1 BiKE enhanced NK cell-mediated apoptosis and depletion of PD-1$^+$ Raji cells, but not PD-1$^-$ Raji cells. Further, PD-1 BiKE induced apoptosis of primary PD-1$^+$ T lymphocytes that are highly relevant to autoimmune disease progression. The BiKE depleted 42% of primary T cells that were stimulated *in vitro*. Importantly, those ablated primary T cells were activated cells. Meanwhile, naive T cells were spared by the BiKE treatment, supporting the crucial selectivity of PD-1 BiKE-directed cell depletion. Lastly, PD-1 BiKE is more effective than a conventional depleting antibody in the depletion of PD-1$^+$ cells. The current work supports PD-1 BiKE is a selective, potent, and safe tool to deplete PD-1$^+$ cells.

*Corresponding author.
E-mail address: mingnan.chen@utah.edu (Mingnan Chen).

Peer review under the responsibility of Chinese Pharmaceutical Association and Institute of Materia Medica, Chinese Academy of Medical Sciences.

https://doi.org/10.1016/j.apsb.2024.10.014

1. Introduction

Bispecific killer cell engagers (BiKEs), a subtype of bispecific antibody, have recently gained popularity for their ability to activate, direct, and release the killing power of effector immune cells such as cytotoxic T cells and natural killer (NK) cells towards target cells. NK cells, crucial members of innate immunity, are potent effector cells of BiKEs due to their early cytokine production and ability to lyse cells without any prior sensitization[1,2].To date, BiKEs that utilize NK cells have achieved remarkable clinical success in cancer treatment[3,4]. We posit that this type of BiKE may be developed to deplete lymphocytes expressing programmed death-1 (PD-1$^+$ cells) and alleviate autoimmune diseases.

PD-1$^+$ cells drive the progression of autoimmune diseases[5-8], and the specific depletion of PD-1$^+$ lymphocytes with an immunotoxin alleviates symptoms in animal models of multiple sclerosis (MS) and type-1 diabetes (T1D)[9,10]. The specific depletion of activated PD-1$^+$ lymphocytes may offer a new therapeutic approach for autoimmune diseases with advantages in safety and efficacy over current therapies, which indiscriminately deplete naïve and activated lymphocytes, compromise lymphocyte repertoires, and lead to long-term, broad immune deficiency[11,12]. For the clinical translation of this therapeutic approach, we initially developed a conventional depleting αPD-1 targeting PD-1$^+$ cells. However, this antibody only showed modest efficacy towards primary PD-1$^+$ lymphocytes that have moderate and dynamic PD-1 expression. The suboptimal outcome may be attributed to an insufficient amount of depleting αPD-1 antibodies per PD-1$^+$ cell to effectively trigger Fc-mediated effector mechanisms, a challenge that BiKEs could overcome. We hypothesized that a BiKE could be used to target PD-1$^+$ lymphocytes and increase NK cell-mediated cytotoxicity towards PD-1$^+$ cells. BiKEs have not yet been utilized as an autoimmune disease therapy, although they are promising for their success in treating HER2-positive breast cancers, Hodgkins lymphoma, Myelodysplastic syndromes, and acute myeloid leukemia, among others[13-17]. In fact, BiKEs have shown superior efficacy compared to their depleting antibody counterparts with minimal sensitivity to antigen expression level[18-20], rendering them an ideal approach to address the aforementioned obstacle of depleting primary PD-1$^+$ cells.

In terms of engaging and activating NK cells through BiKEs, several NK cell receptors have been explored including NKG2D, Nkp46, Nkp30, and CD16[21-23]. Among these receptors, CD16 (FcγRIII), has gained popularity as a BiKE target[24]. CD16 is an activating receptor constitutively expressed by approximately 90% of NK cells. CD16$^+$ NK cells are mature NK cells responsible for inducing antibody-dependent cellular cytotoxicity (ADCC) whereas CD16$^-$ cells are immature and do not contribute to ADCC[25]. ADCC is initiated when CD16 molecules on NK cells recognize the Fcs of antibodies and become clustered. After clustering, adaptor proteins of CD16 become crosslinked where phosphorylation of the immunoreceptor tyrosine-based activation motif (ITAM) activates the NK cells, triggering their degranulation and, ultimately, their lysis of the antibody-coated target cell[25,26]. Though conventional depleting antibodies can induce ADCC through CD16, their mediated ADCC suffers from limitations such as the inherent low-affinity interaction between the Fc of the antibody and CD16, and competition between depleting antibodies and endogenous IgGs for CD16[27]. Because of this, BiKEs have been engineered to bind CD16 with higher specificity and affinity *via* αCD16 variable fragments (Fvs), creating more potent ADCC towards the target cell. This family of CD16 BiKEs has demonstrated tremendous preclinical and clinical success, with several currently in Phase I/II clinical trials[2,28].

The architecture of BiKEs can be chosen based on the application, with general considerations for size, half-life, and stability. Structurally, BiKEs can be broadly categorized as either IgG-like or non-IgG-like based on whether they contain the Fc portion of an IgG. IgG-like BiKEs were first introduced as molecules that resemble a native IgG molecule with an Fc and two Fabs, where each Fab bound a distinct target with monovalence[29]. Further developments have led to tetravalent "appended, IgG-like BiKEs" that are made up of a whole IgG with additional Fvs attached to the Fc, usually *via* flexible amino acid linkers. In this case, the IgG backbone is directed at one antigen with bivalency, and the appended Fvs are directed at the other antigen with bivalency[3,23]. IgG-like BiKEs are, therefore, equal or larger in size compared to native IgG and have similar biological properties in terms of long plasma half-life and overall stability[30]. On the other hand, non-IgG-like BiKEs do not contain an Fc, are smaller in size, and lack any Fc-mediated effector function[30,31]. While IgG-like BiKEs range in molecular weights from 150 to 200 kDa, non-IgG-like BiKEs are typically between 25 and 100 kDa. Due to their larger size and the presence of an Fc, IgG-like BiKEs have elimination half-lives between 2 and 3 weeks, which offers therapeutic advantages in many cases[32]. With smaller molecular weights and the absence of an Fc, non-IgG-like BiKEs have shorter elimination half-lives, ranging from 2 to 11 h[33-35]. Overall, both formats of BiKEs have had success in ablating malignant cells. However, it remains unknown whether non-IgG-like or IgG-like BiKEs are more advantageous in the context of autoimmune diseases as BiKEs have not been examined in these disorders.

Another design consideration of both IgG-like and non-IgG-like BiKEs is how many antigen binding sites they will possess (*i.e.*, their valencies). BiKEs can be bivalent with one binding site for each antigen, or tetravalent with two binding sites for each antigen[23]. As CD16 crosslinking on the NK cell surface is necessary to induce NK cell activation and ADCC, the majority of CD16-targeting BiKEs have been engineered in tetravalent formats[17-19,26,36]. With two CD16 binding sites per molecule, it is hypothesized that tetravalent BiKEs can thus achieve the necessary CD16 crosslinking and NK cell activation more readily than a conventional depleting antibody due to the BiKE' s ability to engage two CD16 molecules at one time[26]. Though some CD16-targeting BiKEs are designed to be bivalent, certain comparisons have shown that the tetravalent counterpart is more effective at inducing NK cell activity towards the target cell[37]. In fact, tetravalent BiKEs may be more favorable as they increase the chances of CD16 binding by utilizing two scFvs as opposed to one.

With these design considerations, we hypothesized that a tetravalent BiKE targeting PD-1 and CD16 (PD-1 BiKE herein) would increase NK cell engagement and potently direct NK cells to deplete PD-1$^+$ cells. We designed PD-1 BiKE in a tetravalent IgG-like format with the intent of engineering a stable, dual-affinity molecule. The resulting PD-1 BiKE demonstrated specific and simultaneous binding to both targets, PD-1 and CD16. Further, PD-1 BiKE successfully induced NK cell-mediated apoptosis and depletion of PD-1$^+$ T and B cells and was more effective than a depleting αPD-1 antibody, consistent with our hypothesis. The current work supports that PD-1 BiKE is a selective and potent molecule to facilitate the depletion of PD-1$^+$ cells, providing a clinically relevant and promising therapeutic for autoimmune diseases.

2. Materials and methods

2.1. Reagents

Expi293 cells were purchased from ThermoFisher (Franklin, MA, USA); Raji-hPD-1 cell line was purchased from Invivogen (San Diego, CA, USA); Apheresis blood cones for isolation of primary human lymphocytes were obtained from the University of Utah ARUP Laboratories. Human NK cell and T cell isolation kits, NK and T cell culturing materials were all purchased from STEMCELL Technologies (Vancouver, BC, Canada). FITC-anti-human CD56 (clone 5.1H11), APC-anti-His (clone J095G-46), APC-anti-human CD107a (clone H4A3), PerCP-anti-human CD3 (clone OKT3); APC-anti-human CD19 (clone H1B19); PE- anti-human CD16 (clone QA1813); PE-anti-human PD-1 (clone EH12.2H7); FITC-anti-human CD69 (clone FN50), anti-human CD16 (clone QA1813) were all purchased from Biolegend (San Diego, CA, USA). Annexin V (Ref. A35110); PI (Ref. P3566); anti-mouse IgG2a-HRP conjugate (Y2a) were purchased from Invitrogen (Eugene, OR, USA); APC-anti-human IgG Fc (G18145) was purchased from BD Biosciences (San Jose, CA, USA). Human CD16a recombinant protein-His (cat. F176) and human PD-1 recombinant protein-mouse Fc Tag (cat. PD-1-H5255) were purchased from AcroBiosystems (Newark, DE, USA); CCK8 metabolic assay (ab228554) was purchased from Abcam (Eugene, OR, USA). SuperSignal ELISA Pico Chemiluminescent Substrate (Ref. 37069) was purchased from ThermoFisher Scientific (Euguene, OR, USA).

2.2. Methods

2.2.1. Cell culture

Raji-hPD-1 cells were cultured in an incubator with 5% CO_2 at 37 °C in RPMI containing 10% FBS, 25 mmol/L HEPES, 1% penicillin−streptomycin, and 100 μg/mL Normocin, according to manufacturer's guidelines. Deidentified blood samples were collected from healthy donors by the ARUP Laboratories and obtained for this study, a procedure that does not need an IRB approval according to policies of the University of Utah. PBMCs were isolated from the blood samples using ficoll density gradient centrifugation. Primary T cells were isolated from PBMCs by magnetic negative selection, then cultured in 5% CO_2 at 37 °C in complete T cell expansion media containing anti-CD3/anti-CD28 cocktail (STEMCELL Technologies, Vancouver, BC, Canada), or cultured in 5% CO_2 at 37 °C in T cell expansion media (STEMCELL Technologies, Vancouver, BC, Canada) with no anti-CD3/anti-CD28 cocktail for unstimulated T cell conditions; Primary NK cells were isolated by magnetic negative selection, and cultured in 5% CO_2 at 37 °C in complete NK cell expansion media (STEMCELL Technologies, Vancouver, BC, Canada). Expi293 cells were cultured in a shaking incubator in 8% CO_2 at 37 °C in BalanCD HEK293 media supplemented with L-glutamine (Irvine Scientific, Santa Ana, CA, USA).

2.2.2. Production of PD-1 BiKE and monoclonal antibodies

Gene sequences for anti-PD-1 antibodies and anti-CD16 variable domains were obtained from published sources[38,39]. For PD-1 BiKE, and anti-PD-1 antibodies heavy and light chain gene sequences were cloned into separate *pcDNA3.1* mammalian expression vectors and plasmids were amplified in *Escherichia coli.* Plasmid DNA was purified using ZymoPURE II Plasmid Midiprep Kit (Irvine, CA, USA). Plasmids were then used to transfect Expi293 cells a 2:1 light chain: heavy chain ratio. After 5 days, cell supernatant was harvested, and proteins were isolated with either Protein G chromatography for mAbs, or SEC for PD-1 BiKE. Purity was assessed with FPLC and SDS-PAGE.

2.2.3. PD-1 BiKE stability assay

PD-1 BiKE was incubated in 5 mL FBS at a concentration of 4 nmol/L at 37 °C for 48 h. At $t = 0$, and $t = 24$ h, 700 μL aliquots were removed and stored at −20 °C. After 48 h, samples were thawed and ELISA was used to quantify the amount of functional BiKE in each sample. For ELISA: a flat-bottom 96-well plate was coated overnight at 4 °C with 150 nmol/L PD-1 protein; wells were blocked with PBS + 1% BSA for 2 h; 100 μL samples from each time point were then incubated for 1 h; wells were washed 3 times with PBS + 0.05% Tween 20, then incubated for 1 h with 80 nmol/L soluble CD16 protein carrying a tag; wells were washed 3 times; anti-His-HRP was added for 1 h; wells were washed 3 times and chemiluminescent substrate was added; luminescence was detected using a Tecan Infinite 200 Pro Microplate Reader.

2.2.4. Target binding assays

2.2.4.1. Flow cytometry. For binding to PD-1, PD-1$^+$ or PD-1$^-$ cells were incubated with 30 nmol/L PD-1 BiKE for 30 min in PBS at 4 °C. Cells were washed twice, then anti-human IgG Fc-APC detection antibody was added for 30 min at 4 °C. Flow cytometry (BD FACS Canto) was used to detect BiKE-bound cells. For simultaneous binding to PD-1 and CD16, PD-1$^+$ cells were incubated with varying concentrations of PD-1 BiKE for 30 min in PBS at 4 °C, washed twice, then 150 nmol/L CD16 soluble protein carrying a His tag was added for 30 min. After two washes, APC-anti-His antibody was added to cells to detect CD16-bound cells, cells were washed, then flow cytometry was used to determine the quantity of cells bound by PD-1 BiKE and CD16 protein.

2.2.4.2. ELISA. A flat-bottom 96-well plate was coated overnight at 4 °C with 150 nmol/L CD16 protein; wells were blocked with PBS + 1% BSA for 2 h; PD-1 BiKE or anti-PD-1 antibodies were added at varying concentrations in PBS + 0.05% Tween 20 + 1% BSA and incubated for 1 h; wells were washed 3 times with PBS + 0.05% Tween 20, then incubated for 1 h with 80 nmol/L soluble PD-1 protein carrying a mouse Fc (IgG2a) tag; wells were washed 3 times; anti-mouse IgG2a-HRP conjugate was added for 1 h; wells were washed 3 times and chemiluminescent substrate was added; luminescence was detected using a Tecan Infinite 200 Pro Microplate Reader.

2.2.5. NK cell activation assays

PD-1$^+$ Raji cells and primary NK cells were seeded at a 2:1 E:T ratio in 400 μL RPMI containing 10% FBS. Varying concentrations of either PD-1 BiKE or depleting αPD-1 were added to respective wells, and plates were incubated at 37 °C with 5% CO_2 for 4 h. Cells were transferred to tubes, washed, then resuspended in PBS + 2% FBS. Cells were stained with FITC-CD56 antibody and APC-CD107a antibody for 30 min at 4 °C. Cells were washed twice, then analyzed with flow cytometry. Cells that stained positive for CD56 and CD107a were characterized as activated NK cells. Mean fluorescence intensities (MFI) were quantified and fold-increase was determined by dividing respective MFIs by the MFI of NK cells co-cultured with Raji in the absence of PD-1 BiKE or depleting αPD-1.

2.2.6. Apoptosis assays

Target cells and primary NK cells were seeded at a 2:1 of *E*:*T* ratio in a 48-well plate in 400 μL RPMI containing 10% FBS with varying concentrations of PD-1 BiKE. Cells were incubated at 37 °C with 5% CO_2 for 4 h. Cells were transferred to tubes, washed, and resuspended in Annexin V binding buffer; FITC-anti-CD56, Annexin V, and PI were incubated with cells for 30 min at 4 °C. Cells were washed twice then analyzed by flow cytometry: cells that stained negative for CD56, and positive for Annexin V, PI, or both were determined to be apoptotic target cells.

2.2.7. Target cell depletion assays

2.2.7.1. Flow cytometry. Target cells and primary NK cells were seeded at varying ratios in a 48-well plate in 400 μL RPMI containing 10% FBS and dosed with various concentrations of PD-1 BiKE, αPD-1 antibodies, or αCD16 antibody. Plates were incubated at 37 °C in 5% CO_2. After 24 h, cells were transferred to tubes, washed, and resuspended in PBS containing 2% FBS. Cells were stained with FITC-anti-CD56 antibody, and either APC-anti-CD19 (Raji cells) or PerCP-anti-CD3 (primary T cells) antibodies for 30 min at 4 °C, then washed twice. Flow cytometry was used to quantify the percentages of NK cells and target cells remaining in each sample after 24 h. For CD69$^+$ T cell depletion assays, target cells and primary NK cells were seeded at varying ratios in a 48-well plate in 400 μL RPMI containing 10% FBS and dosed with various concentrations of PD-1 BiKE or depleting αPD-1. Plates were incubated at 37 °C in 5% CO_2. After 24 h, cells were transferred to tubes, washed, and resuspended in PBS containing 2% FBS. Cells were stained with PerCP-anti-CD3 and FITC-anti-CD69 for 30 min at 4 °C, then washed twice. Flow cytometry was used to quantify the number of total T cells, and CD69$^+$ T cells for each group.

2.2.7.2. CCK-8 assay. Either PD-1$^+$ Raji or WT Raji were seeded at a 1:1 ratio with primary NK cells in a 96-well plate in 200 μL of RPMI containing 10% FBS. Several concentrations of PD-1 BiKE were added to respective wells then plates were incubated at 37 °C in 5% CO_2 for 24 h. CCK8 solution (Abcam, Eugene, OR, USA) was added to each well and incubated at 37 °C for 2 h. Absorbance was read at 450 nm on a colorimetric plate reader.

2.2.8. Intrinsic cytotoxicity of PD-1 BiKE to target cells

PD-1$^+$ Raji, WT Raji, or primary T cells were incubated with varying concentrations of PD-1 BiKE in 200 μL RPMI + 10% FBS. After 24 h, CCK-8 reagent was added and absorbance was read at 450 nm on a colorimetric plate reader to determine cell viability.

2.2.9. Statistical analysis

Analysis of variance (ANOVA) was used to assess the differences among the means of treatment groups followed by multiple comparisons using the Benferroni adjustment when dose−response was examined. Additional two-sample comparisons using a one-sided *t*-test were performed for groups of interest and are reported in figures.

3. Results

3.1. Design and production of PD-1 BiKE

We designed PD-1 BiKE to potentiate the engagement of NK cells and their ADCC directed at autoreactive PD-1$^+$ lymphocytes compared to a conventional depleting αPD-1 (Fig. 1A). The PD-1 BiKE assumed an IgG-scFv configuration[36], comprising a whole αPD-1 backbone, with two CD16-targeting scFvs tethered to the C terminus of the αPD-1 Fc *via* flexible peptide linkers (Fig. 1B). Nivolumab was used as the αPD-1 backbone[38], which belongs to the IgG4 isotype. For the CD16-targeting domains, the V_L and V_H of an anti-human CD16 antibody (clone NM3E2) were used[39]. Two separate plasmids were designed for the expression of PD-1 BiKE (Fig. 1C). The first plasmid encodes an extended heavy chain which, from N to C terminus, contains the heavy chains of nivolumab, the peptide linker $(GGGGS)_3$, the αCD16 V_H, another linker, $(GGGGS)_3$, and the αCD16 V_L (Fig. 1C). The second plasmid encodes the light chain of nivolumab. The PD-1 BiKE has a theoretical molecular weight of approximately 200 kDa.

To express PD-1 BiKE, Expi293 cells were transfected with the aforementioned plasmids at a 2:1 light:heavy chain ratio. Purified BiKE was examined by using size exclusion chromatography and eluted at a position consistent with a globular 200 kDa protein (Fig. 1D). Results of SDS-PAGE confirmed the purity of PD-1 BiKE (Fig. 1E); in the sample treated with reducing loading buffer, there were only two bands present, one at 75 kDa (extended heavy chain) and one at 25 kDa (αPD-1 light chain); in the sample treated with non-reducing buffer, there is only a single band with no impurities present. The SDS-PAGE results of reduced samples also show that the extended heavy chain and the light chain are connected by disulfide bonds. The final yield of PD-1 BiKE was ∼60 mg/L of culture. The stability of PD-1 BiKE under physiological conditions was confirmed with ELISA. After 24 h, 91% of PD-1 BIKE maintained the capacity to bind with PD-1 and CD16 simultaneously; after 48 h, 87% remained with this capacity (Fig. 1F).

3.2. PD-1 BiKE specifically binds to PD-1 and CD16

We investigated the specific binding of PD-1 BiKE to PD-1 using a Raji cell line modified to overexpress PD-1 (PD-1$^+$ Raji) compared to WT Raji, which do not express PD-1 (Supporting Information Fig. S1A). Flow cytometry analysis showed that when incubated with 30 nmol/L PD-1 BiKE, 98% of PD-1$^+$ Raji cells were bound by PD-1 BiKE, a significantly greater percentage compared to WT Raji (Fig. 2A), indicating selectivity of the αPD-1 domain of PD-1 BiKE.

Critical to PD-1 BiKE function is its ability to simultaneously bind PD-1 and CD16. Leveraging the availability of PD-1$^+$ Raji cells, we examined whether PD-1 BiKE that is bound to PD-1$^+$ cells can also bind to CD16. We dosed PD-1$^+$ Raji cells with either 0, 1, 10, or 100 nmol/L PD-1 BiKE, then incubated cells with soluble CD16 carrying a His-tag. Lastly, an anti-His detection antibody was used to detect the number of PD-1$^+$ Raji cells that were bound by CD16 (Fig. S1B). At 1 nmol/L, approximately 28% of PD-1$^+$ Raji were bound to CD16 (Fig. 2B). At 10 nmol/L and 100 nmol/L, the percentages of CD16-bound cells were 78% and 96%, respectively. Compared to the condition where PD-1 BiKE was absent, the association of CD16 to PD-1$^+$ Raji was significantly higher at all three concentrations of PD-1 BiKE. The difference indicates that the binding of CD16 to PD-1$^+$ Raji cells was dependent on PD-1 BiKE. The results also confirm the BiKE's capacity to simultaneously bind PD-1 and CD16.

The next important feature of the PD-1 BiKE design is that its binding to CD16 was primarily due to the αCD16 scFvs of PD-1 BiKE and not the Fc region of its nivolumab backbone. To examine this, we first generated nivolumab in-house and confirmed its binding to PD-1$^+$ cells (Supporting Information Fig. S2A and

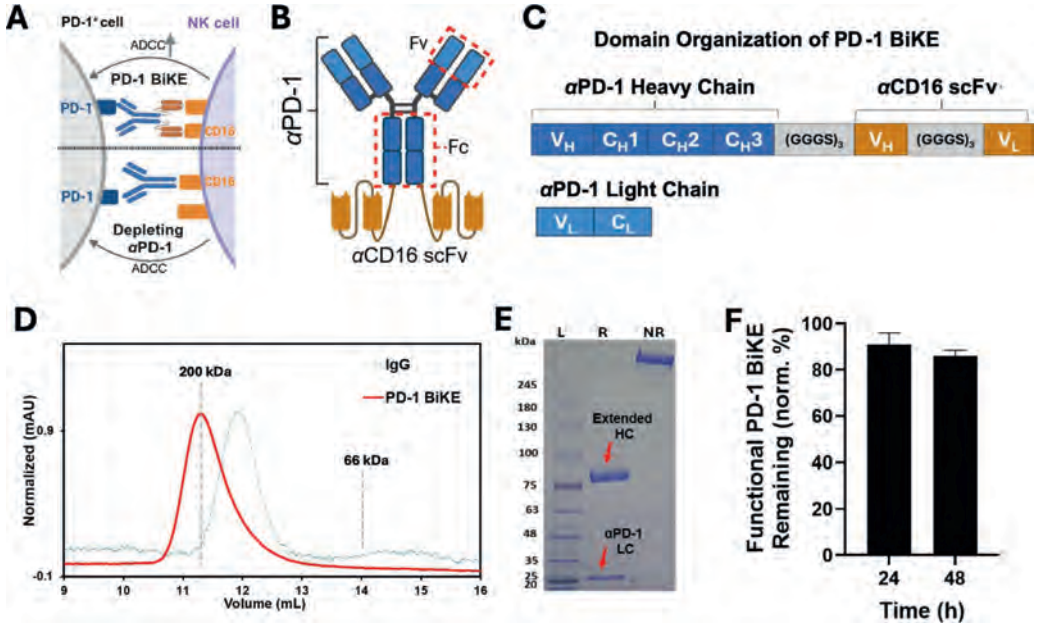

Figure 1 Design and production of PD-1 BiKE. (A) Schematic illustrating the advantage of PD-1 BiKE *versus* a conventional depleting αPD-1 at engaging NK cells, activating them, and directing their cytotoxic activity towards PD-1$^+$ cells; (B) The tetravalent structure of PD-1 BiKE that contains an αPD-1 backbone (nivolumab) with two αCD16 scFvs attached to the Fc *via* flexible amino acid linkers; (C) Schematic depicting the domain organization of PD-1 BiKE, encoded by the genes of two plasmids used to transfect Expi293 cells; (D) SEC chromatogram showing elution of PD-1 BiKE (red line) compared to a depleting antibody (IgG, blue line) at a flow rate of 0.600 mL/min; the elution position of protein markers 200 kDa and 66 kDa are indicated by dashed lines; (E) SDS-PAGE verifying the purity of PD-1 BiKE after it was treated with reducing (R) and non-reducing (NR) loading buffers; after treatment with reducing buffer, the extended heavy chain (HC) of PD-1 BiKE migrates to ~75 kDa while the αPD-1 light chain (LC) migrates to ~25 kDa and confirms that the HC and LC of PD-1 BiKE are connected *via* disulfide bonds; (F) Relative percentages of functional PD-1 BiKE remaining after 24 and 48 h of incubation under physiological conditions; PD-1 BiKE was incubated at 37 °C in serum and aliquots were removed at designated time points, then ELISA was used to quantify the amount of PD-1 BiKE present in the sample that could bind to both PD-1 and CD16. Percentages were calculated by normalizing to PD-1 BiKE signal at $t = 0$. Data are mean ± SD, $n = 4$.

S2B). The binding of PD-1 BiKE *versus* nivolumab to CD16 was compared by ELISA. Here, a 96-well plate was first coated with CD16 protein. Either PD-1 BiKE or nivolumab were incubated in the wells and allowed to interact with the CD16 for 1 h. After incubation, the bound PD-1 BiKE and nivolumab were quantified using soluble PD-1 in combination with an HRP-αPD-1 detection antibody (Fig. 2C). As expected, the binding of PD-1 BiKE to the coated wells was ~43 times greater than that of nivolumab

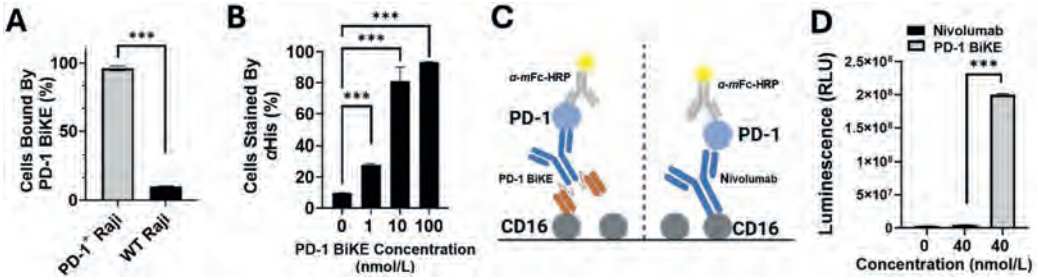

Figure 2 PD-1 BiKE specifically binds to its targets, PD-1 and CD16. (A) PD-1 BiKE binds to PD-1$^+$ Raji cells, but not WT Raji cells; (B) PD-1 BiKE binding to PD-1$^+$ Raji cells and CD16 protein simultaneously; PD-1$^+$ Raji cells were incubated with varying concentrations of PD-1 BiKE, then exposed to CD16 soluble protein carrying a His-Tag; after washing, cells were incubated with an αHis-APC detection antibody; cells that stained positive for αHis-APC were considered associated with CD16; at each concentration of PD-1 BiKE there is a greater percentage of cells associated with CD16 than the condition of 0 nmol/L PD-1 BiKE; (C) Schematic of ELISA design to determine binding to CD16; a 96-well plate was coated with CD16 protein and exposed to either PD-1 BiKE or nivolumab (IgG4), then incubated with PD-1 protein with a mouse Fc tag (mFc), an HRP-conjugated α-mFc detection antibody was used to detect bound antibodies; (D) Luminescence signal produced by PD-1 BiKE is greater than nivolumab (IgG4); Data are mean ± SD, n = 5; t-test ***P < 0.001.

(Fig. 2D). Because the PD-1 binding domains of both PD-1 BiKE and nivolumab are identical, the difference is attributed to the stronger binding to CD16 by PD-1 BiKE than nivolumab.

Altogether, the results show that the produced PD-1 BiKE assumed a conformation that supports its binding domains, underscored by its binding to both PD-1 and CD16. Further, PD-1 BiKE demonstrated a high degree of specificity for PD-1 by its binding selectivity for PD-1$^+$ Raji compared to WT Raji. PD-1 BiKE was able to simultaneously bind both PD-1 and CD16, and it showed greater affinity to CD16 than a conventional antibody.

3.3. PD-1 BiKE induces NK cell-mediated apoptosis and depletion of PD-1$^+$ Raji cells

To determine whether PD-1 BiKE could direct NK cell-mediated cytotoxicity specifically towards PD-1$^+$ cells, we first examined the apoptosis of PD-1$^+$ cells induced by PD-1 BiKE in the presence of NK cells. We employed both PD-1$^+$ Raji and WT Raji as target cells. We found that the presence of PD-1 BiKE at all tested concentrations, ranging from 0.1 to 100 nmol/L, increased the fractions of apoptotic PD-1$^+$ Raji when compared to the result where PD-1 BiKE is absent (Fig. 3A). Further, we found that all concentrations of PD-1 BIKE resulted in more apoptotic PD-1$^+$ Raji cells than WT Raji cells ($P < 0.001$; ANOVA). Indeed, the 0.1 nmol/L concentration of PD-1 BiKE increased the fraction of apoptotic cells to 38% among PD-1$^+$ Raji compared to 25% of WT Raji. The 1 nmol/L concentration of PD-1 BiKE resulted in 39% apoptotic PD-1$^+$ Raji cells while the fraction was only 27% among WT Raji. The higher concentrations of 10 and 100 nmol/L PD-1 BiKE both induced apoptosis among 43% of PD-1$^+$ Raji cells; in contrast, the apoptotic fractions of WT Raji cells remained at the same level as when there was no PD-1 BiKE present (Fig. 3A). Altogether, this result showed that PD-1 BiKE promoted apoptosis in PD-1$^+$ cells.

Next, we sought to evaluate the ability of PD-1 BiKE to induce NK cell-mediated depletion of PD-1$^+$ target cells. Either PD-1$^+$ Raji or WT Raji cells were incubated with NK cells at a 1:1 effector: target (E: T) ratio for 24 h in the presence or absence of 30 nmol/L PD-1 BiKE. The percentages of Raji cells that survived the incubation were determined using flow cytometry. To account for nonspecific killing of target cells by NK cells or cell amplification during the incubation, the percentages of live Raji cells remaining for treatment groups were calculated by normalizing to the percentage of Raji remaining when there was no PD-1 BiKE present. Results show that 22.92% of PD-1$^+$ Raji cells remained after treatment with PD-1 BiKE, meaning that 77.08% of the cells were ablated (Fig. 3B). An example histogram shows that in the absence of PD-1 BiKE, there is a large PD-1$^+$ Raji peak; however, this peak nearly disappears after PD-1 BiKE treatment (Fig. 3C). On the other hand, 95% of the WT Raji cells survived after PD-1 BiKE treatment (Fig. 3B and C). Interestingly, the same level of effect of PD-1 BiKE was also observed when a 5:1 *E*:*T* ratio was used (Supporting Information Fig. S3A and S3B). As target cell depletion was the same for the two ratios, this indicates that PD-1 BiKE is effective at depleting PD-1$^+$ cells even with fewer NK cells present. Importantly, there was no decrease in PD-1$^+$ or WT Raji when incubated with PD-1 BiKE in the absence of NK cells, suggesting that the BiKE has no intrinsic cytotoxicity (Fig. S3C).

We next expanded the aforementioned study by using multiple concentrations of PD-1 BiKE ranging from 0.3 to 30 nmol/L. Here, all concentrations of PD-1 BiKE resulted in significant depletion of PD-1$^+$ Raji compared to the controls without PD-1 BiKE (Fig. 3D). To our surprise, there was no statistically significant dose-dependence observed within the tested concentration range. Even the lowest concentration, 0.3 nmol/L, resulted in only 30% of PD-1$^+$ Raji cells remaining, while the percentages of remaining PD-1$^+$ Raji cells were 26% and 22% for the 3 nmol/L and 30 nmol/L groups, respectively. These results indicated sub-nanomolar potency of PD-1 BiKE. Meanwhile, the potency of PD-1 BiKE was dependent on PD-1 expression of the target cells since, at the 30 nmol/L concentration, there was no reduction in WT Raji cells (Fig. 3D). Further, the importance of bispecificity in the BiKE design was highlighted by the result that PD-1$^+$ Raji cells were not depleted when they were co-cultured with NK cells and an αCD16 antibody instead of PD-1 BiKE (Fig. S3D).

Lastly, we wanted to further expand the PD-1 BiKE concentration range and examine whether its cytotoxicity is concentration-dependent. We determined the cell viability after treatments using a high-throughput, metabolism-based assay (CCK-8). Overall, the treatment with PD-1 BiKE resulted in lower numbers of live PD-1$^+$ Raji cells, reflected by the lower absorbance values of the CCK-8 assay, than live WT Raji ($P < 0.001$; ANOVA) (Fig. 3E). For the PD-1$^+$ Raji cells, there was a clear trend of decreasing absorbance values with increasing concentrations of PD-1 BiKE. When the PD-1 BiKE concentration was above 0.6 nmol/L, the absorbance values plateaued at 0.48, indicating maximum cytotoxicity of PD-1 BiKE in the presence of NK cells. This is consistent with our previous depletion data obtained from flow cytometry (Fig. 3D), where between 0.3 and 30 nmol/L, there was no significant increase in cytotoxicity.

Altogether, the data show that PD-1 BiKE is extremely potent at inducing NK cell-mediated cytotoxicity towards PD-1$^+$ Raji cells and that the effects of PD-1 BiKE are dependent on PD-1.

3.4. PD-1 BiKE induces greater NK cell activation and depletion of PD-1$^+$ Raji cells compared to depleting αPD-1

Because PD-1 BiKE was confirmed to promote NK cell-mediated depletion of PD-1$^+$ cells, we wondered whether PD-1 BiKE would be more effective than a conventional depleting αPD-1 in this capacity. To answer this question, a depleting αPD-1 was produced using the same PD-1 variable domains as PD-1 BiKE (nivolumab), with an IgG1 isotype for the heavy chain constant regions (Supporting Information Fig. S4). After obtaining the αPD-1, we first compared its binding to CD16 to that of PD-1 BiKE and nivolumab using the ELISA format described in Fig. 1C. As expected, PD-1 BiKE demonstrated significantly stronger binding to CD16 than the depleting αPD-1 (Fig. 4A). At 40 nmol/L, PD-1 BiKE produced 6 times more signal than depleting αPD-1. In fact, at every tested concentration, PD-1 BiKE resulted in higher luminescence than depleting αPD-1. Even the lowest concentration of 0.3 nmol/L PD-1 BiKE produced 2.5 times greater signal than 40 nmol/L depleting αPD-1. These results support that PD-1 BiKE has stronger binding to CD16 than the Fc of the depleting αPD-1. Lastly, the depleting αPD-1 (IgG1) produced $\sim$2 times more signal than the nivolumab (IgG4) control (Fig. 4A), consistent with the Fc of IgG1's higher affinity for CD16 than the Fc of IgG4[40].

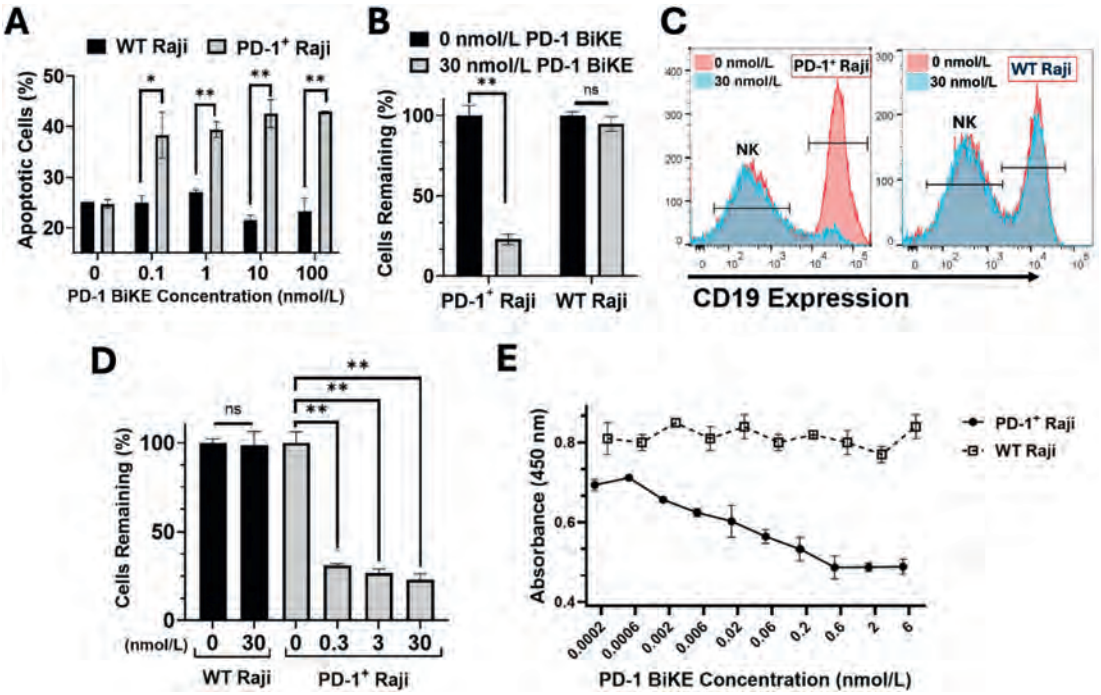

Figure 3 PD-1 BiKE effectively mediates apoptosis and depletion of PD-1$^+$ Raji cells. (A) Percentages of apoptotic PD-1$^+$ Raji cells *vs.* WT Raji after 4-h of co-culture with NK cells; at all concentrations tested PD-1 BiKE induced more apoptosis in PD-1$^+$ Raji compared to WT Raji; (B) Percentages of PD-1$^+$ Raji *vs.* WT Raji remaining after 24 h of co-culture with NK cells at a 1:1 *E*:*T* ratio with or without 30 nmol/L PD-1 BiKE; treatment with PD-1 BiKE resulted in greater depletion of PD-1$^+$ Raji cells compared to WT Raji; (C) Representative flow cytometry histograms showing PD-1$^+$ Raji, WT Raji, and NK cell populations after 24 h with or without 30 nmol/L PD-1 BiKE; when treated with PD-1 BiKE, the PD-1$^+$ Raji population is reduced while the WT Raji population remains the same as when there is no PD-1 BiKE present; (D) Percentages of PD-1$^+$ Raji or WT Raji remaining after 24 h of co-culture with NK cells at a 1:1 E:T ratio with varying concentrations of PD-1 BiKE; each concentration of PD-1 BiKE tested reduced the PD-1$^+$ Raji cell fraction while the highest PD-1 BiKE concentration had no effect on WT Raji; (E) Absorbance values from CCK-8 assay with either PD-1$^+$ Raji or WT Raji after 24 h of co-culture with NK cells at a 1:1 *E*:*T* ratio with varying concentrations of PD-1 BiKE; PD-1 BiKE treatment resulted in lower absorbance values for PD-1$^+$ Raji cells at all concentrations compared to WT Raji. Data are mean ± SD, $n = 3$; *t*-test $^*P < 0.05$, $^{**}P < 0.01$, and $^{***}P < 0.001$; ns, not significant. Percentages shown in (B) and (D) are normalized to respective 0 nmol/L PD-1 BiKE groups.

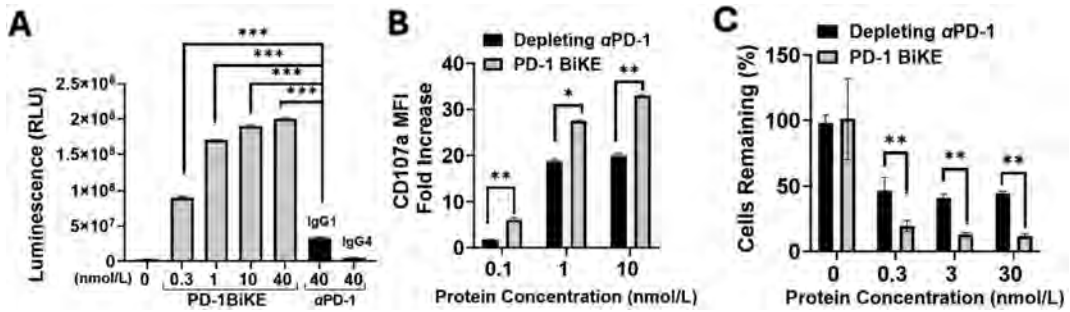

Figure 4 PD-1 BiKE is more effective at inducing NK cell activation and depletion of PD-1$^+$ target cells compared to depleting αPD-1 (IgG1). (A) ELISA results showing binding to CD16 by PD-1 BiKE, depleting αPD-1 (IgG1), and nivolumab (IgG4); each concentration of PD-1 BiKE produced higher luminescence signal compared to the depleting αPD-1; (B) CD107a expression on NK cells induced by PD-1 BiKE *vs*. depleting αPD-1; all concentrations of PD-1 BiKE induced a greater fold increase in CD107a expression compared to the depleting αPD-1; (C) PD-1$^+$ Raji cells remaining after 24 h of co-culture with NK cells at a 1:1 ratio in the presence or absence of varying concentrations of PD-1 BiKE or depleting αPD-1; fractions of PD-1$^+$ Raji were significantly lower when treated with PD-1 BiKE at all concentrations tested. Data are mean ± SD, $n = 4$ (A), $n = 3$ (B, C); *t*-test $^*P < 0.05$, $^{**}P < 0.01$, and $^{***}P < 0.001$. Percentages shown in (C) are normalized to respective 0 nmol/L PD-1 BiKE groups.

We next examined whether PD-1 BiKE would induce greater NK cell activation than the depleting αPD-1. Co-cultures of PD-1$^+$ Raji cells and NK cells were treated with PD-1 BiKE, depleting αPD-1, or medium only. The activation of NK cells was measured by CD107a expression. Overall, PD-1 BiKE induced greater CD107a expression on NK cells than depleting αPD-1 ($P < 0.05$; ANOVA) (Fig. 4B). Compared to the medium only-treated co-cultures, 0.1 nmol/L PD-1 BiKE resulted in a six-fold increase in NK cell CD107a expression, while 0.1 nmol/L depleting αPD-1 only increased the expression by one-fold. Interestingly, there was only a slight increase in CD107a expression between 1 nmol/L and 10 nmol/L of depleting αPD-1 (18- and 19-fold higher than medium-treated, respectively). However, the difference was drastic between 1 nmol/L PD-1 BiKE and 10 nmol/L BiKE, 27- *versus* 33-fold higher than the medium-treated co-culture. The higher CD107a expression observed after PD-1 BiKE treatment suggests that the PD-1 BiKE is more effective than the depleting αPD-1 at activating NK cells.

Lastly, we examined whether PD-1 BiKE is also more potent than the depleting αPD-1 for the depletion of PD-1$^+$ cells. PD-1$^+$ Raji cells were seeded with NK cells and given 0.3−30 nmol/L doses of either PD-1 BiKE or depleting αPD-1. Overall, PD-1 BiKE resulted in a greater reduction of PD-1$^+$ Raji cells compared to the depleting αPD-1 ($P < 0.001$; ANOVA) (Fig. 4C). As low as 0.3 nmol/L PD-1 BiKE reduced the percentage of PD-1$^+$ Raji cells to 19.6%, whereas 0.3 nmol/L depleting αPD-1 only reduced PD-1$^+$ Raji cells to 46.5%. When treated with 3 nmol/L and 30 nmol/L PD-1 BiKE, the percentages of remaining PD-1$^+$ Raji cells were less than 15%, on average. In contrast, the remaining PD-1$^+$ Raji cells were 41% and 45%, respectively, after treatments with 3 and 30 nmol/L of depleting αPD-1.

In conclusion, PD-1 BiKE demonstrated stronger capacities than the depleting αPD-1 in binding to CD16, NK cell activation, and the depletion of PD-1$^+$ Raji cells.

3.5. PD-1 BiKE induces apoptosis and NK cell-mediated depletion of PD-1$^+$ primary T cells

To investigate whether PD-1 BiKE could induce NK cell activation when the target cells are primary PD-1$^+$ cells, we subjected primary human T cells to stimulating conditions using αCD3 and αCD28 to induce their PD-1 expression. Approximately 50%−60% of primary T cells that received stimulating treatment (herein T_{+STIM} sample) became PD-1$^+$ (Fig. 5A). In contrast, 88.5% of primary T cells without stimulation (T_{UNSTIM} sample) are PD-1$^-$, with a very small fraction (∼12.5%) expressing PD-1 (Fig. 5A).

We used the T_{+STIM} and T_{UNSTIM} samples to investigate whether PD-1 BiKE could bind to primary PD-1$^+$ cells selectively. For the cells in the T_{+STIM} samples, approximately 60% were bound to PD-1 BiKE, while there was no significant binding to the cells in the T_{UNSTIM} samples (Fig. 5B). Further, we examined the simultaneous binding by PD-1 BiKE to T_{+STIM} cells and CD16 protein with the same methods described in Fig. S1B. We conducted the study with PD-1 BiKE concentrations ranging from 0 to 250 nmol/L and found dose-dependent association of CD16 with T_{+STIM} cells. At a 25 nmol/L dose of PD-1 BiKE, 36% of T_{+STIM} cells stained positive for the detection antibody, suggesting that they were associated with CD16 (Fig. 5C), compared to less than 1% when there was no PD-1 BiKE present. At 50 nmol/L PD-1 BiKE, the percentage of CD16-associated cells increased to 40%, while at 250 nmol/L PD-1 BiKE, that percentage was 56%. This data shows that the association of CD16 with T_{+STIM} cells is dependent on PD-1 BiKE and further suggests that PD-1 BiKE simultaneously binds primary PD-1$^+$ cells and CD16.

Next, we investigated whether PD-1 BiKE could induce NK cell-mediated apoptosis towards cells in the T_{+STIM} samples. In the co-culture of T_{+STIM} and NK cells, 1 nmol/L PD-1 BiKE induced apoptosis in 24.6% of T_{+STIM} cells compared to 15.1% of cells without any PD-1 BiKE present (Fig. 5D). The 5 nmol/L dose of PD-1 BiKE induced apoptosis in 30.1% of T_{STIM} cells, a two-fold increase from the group with no PD-1 BiKE present (Fig. 5D). The data supports the hypothesis that PD-1 BiKE can direct NK cells to induce apoptosis in primary PD-1$^+$ cells.

Finally, we examined whether the BiKE could also augment the depletion of primary PD-1$^+$ cells by NK cells. To answer this question, we measured T (CD3$^+$) cell numbers in the NK and T_{+STIM} cell mixtures after treatments and compared them to T cell numbers in the cell mixture without BiKE. Since the detecting αPD-1 and PD-1 BiKE compete for PD-1, we were not able to count the number of PD-1$^+$ cells directly after the BiKE treatment. Instead, we quantified the fractions of total T cells in the T_{+STIM} and T_{UNSTIM} samples after PD-1 BiKE treatment. T_{+STIM} cells were co-cultured with NK cells at two *E*:*T* ratios, 1:1 or 5:1. At a 1:1 ratio, PD-1 BiKE reduced T_{+STIM} cells to 70.4% as compared to treatment groups without BiKE, indicating the reduction of 29.6% of T_{+STIM} cells (Fig. 5E and F). At the 5:1 ratio, there was a 38% reduction (Fig. 5E and F). Since T_{+STIM} cells are composed of both PD-1$^+$ and PD-1$^-$ T cells (Fig. 5A), complete ablation of T_{+STIM} cells is neither expected nor desired, as that would indicate depletion of PD-1$^-$ T cells as well. In fact, when T_{UNSTIM} samples, which consist of primarily PD-1$^-$ cells, were used for this study, the treatment of PD-1 BiKE did not significantly reduce T cell numbers (Supporting Information Fig. S5A), highlighting the correlation of PD-1 expression with the efficacy of PD-1 BiKE. Consistent with our previous data with PD-1$^+$ Raji cells, PD-1 BiKE is also more potent than the depleting αPD-1 in the depletion of primary PD-1$^+$ T cells (Fig. S5B).

Since the ultimate goal of depleting PD-1$^+$ cells is to remove activated lymphocytes in autoimmune diseases, we wondered if PD-1 BiKE indeed reduced the number of activated T cells in the T_{+STIM} samples. For this, we exploited CD69, a marker of activated T cells. The expression of CD69 correlates with PD-1 expression among T_{+STIM} cells (Fig. S5C). After treatment with PD-1 BiKE, there were an average of 560 CD69$^+$ T cells remaining per well of a 48-well plate, a significant decrease compared to the average of 999 CD69$^+$ T cells remaining per well when there was no BiKE present (Fig. 5G). Meanwhile, PD-1 BiKE did not significantly reduce the CD69$^-$ T cell population (Fig. 5H). This reinforces the conclusion that PD-1 BiKE can selectively induce the depletion of activated primary T cells while sparing inactivated primary cells.

Altogether, PD-1 BiKE binds to primary PD-1$^+$ T cells and CD16 simultaneously and induces NK cell-mediated cytotoxicity towards primary PD-1$^+$ cells, illustrated by both apoptosis and depletion assays. Importantly, PD-1 BiKE selectively induced the depletion of activated but not inactivated primary T cells.

4. Discussion

PD-1 BiKE was designed to assume an IgG-like configuration and be tetravalent with two binding sites for PD-1 and two for CD16. The structure and design were proven effective based on the characterization results of the BiKE. PD-1 BiKE demonstrated a

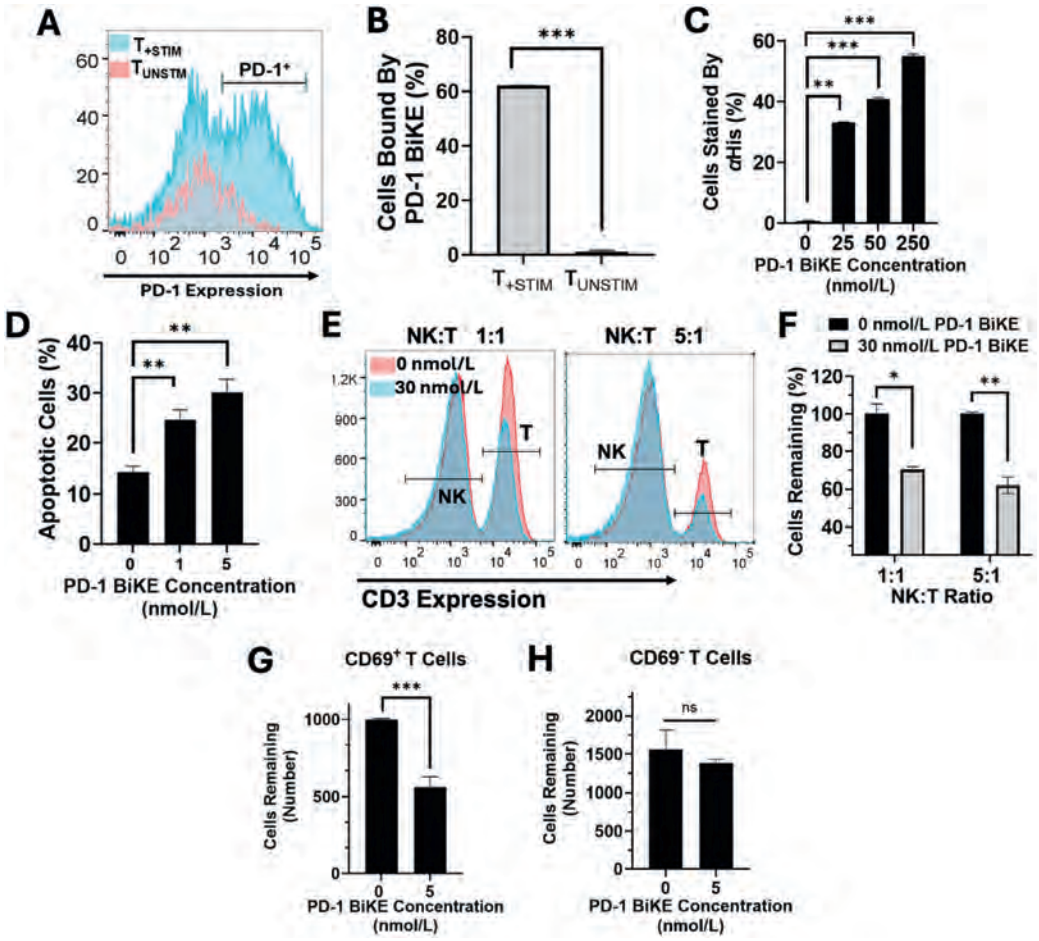

Figure 5 PD-1 BiKE binds to PD-1$^+$ primary T cells and induces their apoptosis and depletion *via* NK cell-mediated cytotoxicity. (A) Representative flow cytometry histogram showing the PD-1 expression of primary T cells stimulated with αCD3 and αCD28 (T_{+STIM}) *vs.* unstimulated primary T cells (T_{UNSTIM}); (B) PD-1 BiKE binds to T_{+STIM} cells but not to T_{UNSTIM} cells; (C) PD-1 BiKE binds to primary PD-1$^+$ cells and CD16 protein simultaneously; T_{+STIM} cells were incubated with varying concentrations of PD-1 BiKE, washed, then incubated with CD16 soluble protein carrying a His-Tag, after washing, cells were incubated with an αHis-APC antibody and analyzed for simultaneous binding to PD-1 and CD16 by flow cytometry; (D) Percentages of apoptotic T_{+STIM} cells after 4 h of incubation with varying concentrations of PD-1 BiKE and NK cells at a 1:1 ratio; when given either 1 or 5 nmol/L PD-1 BiKE the percentage of apoptotic T cells increased compared to 0 nmol/L PD-1 BiKE; (E) Representative flow cytometry gating showing the number of T_{+STIM} cells remaining after 24 h of co-culture with NK cells with or without 30 nmol/L PD-1 BiKE at either 1:1 or 5:1 E:T ratios; at both ratios, the T cell population is smaller when treated with PD-1 BiKE compared to when there is no PD-1 BiKE present; (F) Data summarizing results from (E); at both ratios, there is a significant reduction in total T cells when incubated with 30 nmol/L PD-1 BiKE compared to the groups when PD-1 BiKE is absent; (G) Numbers of CD69$^+$ T cells remaining after coculture of T_{+STIM} cells with NK cells at a 1:1 ratio in the presence or absence of 5 nmol/L PD-1 BiKE; CD69$^+$ T cells were investigated as they constitute the fraction of T_{+STIM} cells that are activated T cells; PD-1 BiKE significantly reduced the number of CD69$^+$ T cells compared to when there is no PD-1 BiKE present; (H) Number of CD69$^-$ T cells remaining after co-culture of T_{+STIM} cells with NK cells and PD-1 BiKE; PD-1 BiKE had no significant effect on CD69$^-$ T cells, representing those that are inactivated T cells. Data are mean ± SD; $n = 4$ (B, C), $n = 3$ (D−J), *t*-test $^*P < 0.05$, $^{**}P < 0.01$, and $^{***}P < 0.001$; ns, not significant. Percentages shown in (F) are normalized to 0 nmol/L PD-1 BiKE groups.

high degree of binding specificity for PD-1$^+$ cells, whether the PD-1$^+$ cells were cell lines (high and constant PD-1 expression) or primary T cells (moderate and dynamic PD-1 expression). PD-1 BiKE bound with both PD-1 and CD16 simultaneously. Furthermore, PD-1 BiKE was able to activate NK cells in the presence of PD-1$^+$ cells, which is attributed to the "engager" function of the BiKE. It is noteworthy the NK cells are only activated by the co-presence of PD-1 BiKE and PD-1$^+$ cells (Fig. 3A), not by one of these two factors, highlighting a controlled and specific activation condition. Consistent with the NK cell activation results, PD-1 BiKE induced specific NK-cell mediated cytotoxicity to PD-1$^+$ cells. Additionally, the extent of the cytotoxicity was dependent on BiKE concentrations. Interestingly, the effect of the BiKE was so intensive, that even picomolar amounts of BiKE cause salient cytotoxicity to PD-1$^+$ cells (Fig. 3E). Another important design of PD-1 BiKE is its use of αCD16 scFVs to engage with CD16 of NK cells, even though the Fc within the BiKE can also interact with the CD16. Our data confirmed this design aspect since the

interactions between the BiKE and CD16 were primarily due to the scFvs, and not the Fc of the BiKE (Fig. 1D). This confirmation is critical as the intended function of PD-1 BiKE is to potentiate engagement with NK cells by possessing two high-affinity αCD16 scFvs compared to the single Fc, which only has moderate affinity to CD16[40,41].

A driving factor of this project is to develop a PD-1$^+$ cell-targeted, depleting agent that is more effective than conventional depleting antibodies. This need was met according to comparisons between PD-1 BiKE and the depleting IgG1 αPD-1. First, PD-1 BiKE showed higher binding affinity to CD16 compared to the depleting αPD-1. Further, PD-1 BiKE demonstrated superior efficacy over the depleting antibody when used to ablate both PD-1$^+$ Raji cells and PD-1$^+$ primary T cells. Consistent with other reports[18,24,36], our data reinforce that bivalent, specific targeting of NK cells *via* CD16 is a useful strategy to harness and enhance their cytotoxic activity compared to conventional depleting antibodies. The superiority of BiKEs over conventional depleting antibodies has a great implication for autoimmune disease treatments as these types of therapies generally have a higher bar for safety than cancer treatments. Similar to monoclonal antibodies, BiKEs have favorable safety profiles[42] and may hold greater promise in clinical translations than immunotoxins, which we have previously used for PD-1$^+$ cell depletion[9,10], though the immunotoxins are advantageous for direct and simple working mechanisms.

Our data clearly show that PD-1 BiKE directed the cytotoxicity of NK cells towards PD-1$^+$ lymphocytes but spared PD-1$^-$ cells (Figs. 3 and 5). Additionally, the treatment of PD-1 BiKE reduced activated primary T cells but not inactivated T cells. These results reinforce one important advantage of targeting PD-1$^+$ cells as a treatment of autoimmune diseases, which is its confined immunosuppression and hence, safety. Current therapies such as ocrelizumab (αCD20) or teplizumab (αCD3) indiscriminately deplete B and T cell populations regardless of activation status. These therapies cause long-term lymphopenia[12,43] and immune deficiency, elevating patients' susceptibility to infections and malignancies[44]. In contrast, PD-1 is only expressed on activated, effector lymphocytes but not naïve lymphocytes[45]. Thus, depleting PD-1$^+$ cells reduces activated lymphocytes (Fig. 5G) and halts the progression of autoimmune diseases[46], while preserving naive lymphocytes and maintaining lymphocyte repertoires. The saved repertoires can then give rise to activated lymphocytes upon immune stimulation and protect treated patients from future infection and malignancy after the depleting agents for PD-1$^+$ cells are cleared. Thus, although depleting PD-1$^+$ cells could cause acute immunosuppression when the depleting agents are in the body, the suppression would be lifted when the depleting agents are gone. The PD-1$^+$ cell depletion is therefore not expected to cause the long-term lymphopenia and immunodeficiency that plague current autoimmune diseases therapeutics like ocrelizumab and templizumab, a distinction that is supported by the results of PD-1 BiKE.

The reported PD-1 BiKE starts an intriguing exploration into the development and application of the BiKE approach in autoimmune disease treatments. To date, the majority of reported BiKEs have shown tremendous clinical and preclinical success as anti-cancer therapies, though it is entirely unknown whether BiKEs can be successfully utilized in treating autoimmune diseases. There are several factors that may demand entirely new considerations and designs when using BiKEs in autoimmune diseases: (i) the immune environment of autoimmune diseases, which is different from cancer; (ii) the target cells of BiKE are primary lymphocytes in autoimmune diseases while the target cells in cancer are tumor cells; (iii) the target antigens in autoimmune diseases, such as PD-1, have dynamic and moderate expression while tumor antigens in cancer often have high and consistent expression. The unknown and new conditions around BiKEs in autoimmune diseases inspire extensive investigations in the future and could bring unprecedented insights. The PD-1 BiKE described here provides an important tool for such investigation and demonstrates the feasibility of depleting primary lymphocytes by BiKEs.

5. Conclusions

In summary, we produced and purified an IgG-like tetravalent BiKE targeting PD-1 and CD16 for the specific depletion of PD-1$^+$ cells. We found that PD-1 BiKE specifically bound to both PD-1 and CD16 independently, and simultaneously. PD-1 BiKE effectively engages NK cells and directs their cytotoxicity towards PD-1$^+$ cells, demonstrated by the depletion of the PD-1$^+$ Raji cell line and primary PD-1$^+$ T cells. PD-1 BiKE is a potent and selective tool for the depletion of PD-1$^+$ cells, presenting a powerful and clinically viable molecule for the treatment of autoimmune diseases.

Acknowledgments

The work was primarily supported by the HCI Melanoma Center Grant, the National Institutes of Health AI139535 grant, and the National Multiple Sclerosis Society GR-1807-31630 grant to Mingnan Chen (USA). We recognize the Core Facility of University of Utah for the service of flow cytometry. We recognize ARUP laboratories for their services in providing healthy donor blood samples. We appreciate Dr. Thomas Gambles and Tony Pomicter for their assistance in the isolation of PBMCs and primary cell culture.

Author contributions

Lauren C. Naatz: Writing − review & editing, Writing − original draft, Methodology, Investigation, Formal analysis. Shuyun Dong: Writing − review & editing, Investigation, Conceptualization. Brian Evavold: Writing − review & editing, Conceptualization. Xiangyang Ye: statistics, writing—review and editing. Mingnan Chen: Writing − review & editing, Supervision, Methodology, Investigation, Funding acquisition, Formal analysis.

Conflicts of interest

The authors declare no conflict of interest.

Appendix A. Supporting information

Supporting information to this article can be found online at https://doi.org/10.1016/j.apsb.2024.10.014.

References

1. Bryceson YT, Chiang SCC, Darmanin S, Fauriat C, Schlums H, Theorell J, et al. Molecular mechanisms of natural killer cell activation. *J Innate Immun* 2011;**3**:216−26.
2. Zhang M, Lam KP, Xu S. Natural killer cell engagers (NKCEs): a new frontier in cancer immunotherapy. *Front Immunol* 2023;**14**: 1207276.
3. Tapia-Galisteo A, Álvarez-Vallina L, Sanz L. Bi- and trispecific immune cell engagers for immunotherapy of hematological malignancies. *J Hematol Oncol* 2023;**16**:83.
4. Moon D, Tae N, Park Y, Lee S-W, Kim DH. Development of bispecific antibody for cancer immunotherapy: focus on T cell engaging antibody. *Immune Net* 2022;**22**:e4.
5. Hughes J, Vudattu N, Sznol M, Gettinger S, Kluger H, Lupsa B, et al. Precipitation of autoimmune diabetes with anti-PD-1 immunotherapy. *Diabetes Care* 2015;**38**:55−7.
6. Ansari M, Salama A, Chitnis T, Smith R, Yagita H, Akiba H, et al. The programmed death-1 (PD-1) pathway regulates autoimmune diabetes in nonobese diabetic (NOD) mice. *J Exp Med* 2003;**198**: 63−9.
7. Salama A, Chitnis T, Imitola J, Ansari M, Akiba H, Tushima F, et al. Critical role of the programmed death-1 (PD-1) pathway in regulation of experimental autoimmune encephalomyelitis. *J Exp Med* 2003;**198**: 71−8.
8. Liang S, Latchman Y, Buhlmann J, Tomczak M, Horwitz B, Freeman G, et al. Regulation of PD-1, PD-L1, and PD-L2 expression during normal and autoimmune responses. *Eur J Immunol* 2003;**33**: 2706−16.
9. Zhao P, Wang P, Dong S, Zhou Z, Cao Y, Yagita H, et al. Depletion of PD-1-positive cells ameliorates autoimmune disease. *Nat Biomed Eng* 2019;**3**:292−305.
10. Zhang T, Dong S, Zhai Y, Naatz L, Zhou Z, Chen M. Diphtheria toxin-derived, anti-PD-1 immunotoxin, a potent and practical tool to selectively deplete PD-1 positive cells. *Protein Sci* 2023;**32**:e4741.
11. Jung S, Kim WU. Targeted immunotherapy for autoimmune disease. *Immun Net* 2022;**22**:e9.
12. Ragonese P, Aridon P, Vazzoler G, Mazzola MA, Lo Re V, Lo re M, et al. Association between multiple sclerosis, cancer risk, and immunosuppressant treatment: a cohort study. *BMC Neurol* 2017;**17**: 155.
13. Singer H, Kellner C, Lanig H, Aigner M, Stockmeyer B, Oduncu F, et al. Effective elimination of acute myeloid leukemic cells by recombinant bispecific antibody derivatives directed against CD33 and CD16. *J Immunother* 2010;**33**:599−608.
14. Gleason M, Ross J, Warlick E, Lund T, Verneris M, Wiernik A, et al. CD16xCD33 bispecific killer cell engager (BiKE) activates NK cells against primary MDS and MDSC CD331 targets. *Blood* 2014;**123**: 3016−26.
15. Hombach A, Jung W, Pohl C, Renner C, Sahin U, Schmits R, et al. A CD16/CD30 bispecific monoclonal antibody induces lysis of Hodgkin's cells by unstimulated natural killer cells *in vitro* and *in vivo*. *Int J Cancer* 1993;**55**:830−6.
16. Kasuya K, Motohide S, Suzuki M, Itoi T, Aoki T, Tsuchida A. Bispecific anti-HER2 and CD16 single-chain antibody production prolongs the use of stem cell-like cell transplantation against HER2-overexpressing cancer. *Int J Mol Med* 2009;**25**:209−15.
17. Schmohl J, Gleason M, Dougherty P, Miller J, Vallera D. Heterodimeric bispecific single chain variable fragments (scFv) killer engagers (BiKEs) enhance NK-cell activity against CD133+ colorectal cancer cells. *Targ Oncol* 2016;**11**:353−61.
18. Ramadoss N, Zhao N, Richardson B, Grant P, Kim P, Blish C. Enhancing natural killer cell function with pg41-targeting bispecific antibodies to combat HIV infection. *AIDS* 2020;**34**: 1313−23.
19. Wu J, Fu J, Zhang M, Liu D. AFM13: a first-in-class tetravalent bispecific anti-CD30/CD16A antibody for NK cell-mediated immunotherapy. *J Hematol Oncol* 2015;**8**:1−4.
20. Li W, Wu Y, Kong D, Yang H, Wang Y, Shao J, et al. One-domain CD4 fused to human anti-CD16 antibody domain mediates effective killing of HIV-1-infected cells. *Sci Rep* 2017;**7**: 9130.
21. Märklin M, Hagelstein I, Koerner SP, Rothfelder K, Pfluegler MS, Schumacher A, et al. Bispecific NKG2D-CD3 and NKG2D-CD16 fusion proteins for induction of NK and T cell reactivity against acute myeloid leukemia. *J Immunother Cancer* 2019;**7**:1−15.
22. Montaldo E, Zotto GD, Chiesa MD, Mingari MC, Moretta A, Maria AD, et al. Human NK cell receptors/markers: a tool to analyze NK cell development, subsets and function. *Cytometry Part A* 2013; **83A**:702−13.
23. Pinto S, Pahl J, Schottelius A, Carter PJ, Koch J. Reimagining antibody-dependent cellular cytotoxicity in cancer: the potential of natural killer cell engagers. *Trends Immunol* 2022;**43**:932−46.
24. Capuano C, Pighi C, Battella S, De Federicis D, Galandrini R, Palmieri G. Harnessing CD16-mediated NK cell functions to enhance therapeutic efficacy of tumor-targeting mAbs. *Cancers* 2021; **13**:2500.
25. Cooper MA, Fehniger TA, Caligiuri MA. The biology of human natural killer-cell subsets. *Trends Immunol* 2001;**22**:633−40.
26. Oostindie SC, Lazar GA, Schuurman J, Parren P. Avidity in antibody effector functions and biotherapeutic drug design. *Nat Rev Drug Discov* 2022;**21**:715−35.
27. Chames P, Van Regenmortel M, Weiss E, Baty D. Therapeutic antibodies: successes, limitations and hopes for the future. *Br J Pharmacol* 2009;**157**:220−33.
28. Myers J, Miller J. Exploring the NK cell platform for cancer immunotherapy. *Nat Rev Clin Oncol* 2021;**18**:85−100.
29. Wang Q, Chen Y, Park J, Liu X, Hu Y, Wang T, et al. Design and production of bispecific antibodies. *Antibodies* 2019;**8**:43.
30. Brinkmann U, Kontermann R. The making of bispecific antibodies. *mAbs* 2017;**9**:182−212.
31. Ma J, Mo Y, Tang M, Shen J, Qi Y, Zhao W, et al. Bispecific antibodies: from research to clinical application. *Front Immunol* 2021;**12**: 626616.
32. Trivedi A, Stienen S, Zhu M, Li H, Yuraszeck T, Gibbs J, et al. Clinical pharmacology and translational aspects of bispecific antibodies. *Clin Transl Sci* 2017;**10**:147−62.
33. Rathi C, Meibohm B. Clinical pharmacology of bispecific antibody constructs. *J Clin Pharmacol* 2015;**55**:21−8.
34. Niu J, Weriong W, Ouellet D. Mechanism-based pharmacokinetic and pharmacodynamic modeling for bispecific antibodies: challenges and opportunities. *Expert Rev Clin Pharmacol* 2023;**16**:977−90.
35. Golay JM. Regazzi. Key features defining the disposition of bispecific antibodies and their efficacy in vivo. *Ther Drug Monit* 2020;**42**: 56−63.
36. Coloma MJ, Morrison SL. Design and production of novel tetravalent bispecific antibodies. *Nat Biotech* 1997;**15**:159−63.
37. Reusch U, Burkhardt C, Fucek I, Le Gall F, Le Gall M, Hoffmann K, et al. A novel tetravalent bispecific TandAb (CD30/CD16A) efficiently recruits NK cells for the lysis of CD30+ tumor cells. *mAbs* 2014;**6**: 727−38.
38. The International Immunogenetics Information System. IMGT/2D Structure-DB card for INN 9623. Available from: https://imgt.org/3Dstructure-DB/cgi/details.cgi?pdbcode=9623.
39. McCall A, Adams G, Amoroso A, Nielson U, Zhang L, Horak E, et al. Isolation and characterization of an anti-CD16 single-chain Fv fragment and construction of an anti-HER2/neu/anti-CD16 bispecific scFv that triggers CD16-dependent tumor cytolysis. *Mol Immunol* 1999;**36**: 433−46.

40. Taeye S, Bentlage A, Mebius M, Meesters J, Vidarsson G. FcγR binding and ADCC activity of human IgG allotypes. *Front Immunol* 2020;**11**:740.
41. Vidarsson G, Dekkers G, Rispens T. IgG subclasses and allotypes: from structure to effector functions. *Front Immunol* 2014; **5**:520.
42. Huan T, Guan B, Li H, Tu X, Zhang C, Tang B. Principles and current clinical landscape of NK cell engaging bispecific antibody against cancer. *Hum Vaccin Immunother* 2023;**19**:2256904.
43. Goldenberg M. Multiple sclerosis review. *Pharm Thera* 2012;**37**: 175−84.
44. Wang L, Wang F, Gershwin M. Human autoimmune diseases: a comprehensive update. *J Int Med* 2015;**278**:369−95.
45. Yao S, Chen L. PD-1 as an immune modulatory receptor. *Cancer J* 2014;**20**:262−4.
46. Cui J, Xu H, Yu J, Ran S, Zhang X, Li Y, et al. Targeted depletion of PD-1-expressing cells induces immune tolerance through peripheral clonal deletion. *Sci Immunol* 2024;**9**:eadh0085.